Subtilase SBT5.2 counterbalances flagellin immunogenicity in the plant apoplast

Pierre Buscaill[1,4], Nattapong Sanguankiattichai[1], Farnusch Kaschani[2], Jie Huang[1], Yuge Li[1,3], Joy Lyu[1], Daniela J. Sueldo[1,5], Markus Kaiser[2] and Renier A. L. van der Hoorn[1*]

[1] The Plant Chemetics Laboratory, Department of Biology, University of Oxford, OX1 3RB, Oxford, United Kingdom

[2] ZMB Chemical Biology, Faculty of Biology, University of Duisburg-Essen, Essen, Germany

[3] Guangdong Provincial Key Laboratory of Applied Botany and State Key Laboratory of Plant Diversity and Prominent Crops, South China Botanical Garden, Chinese Academy of Sciences, Guangzhou 510650, China.

[4] Current address: School of Biological Sciences, University of Bristol, BS8 1TQ, Bristol, United Kingdom

[5] Current address: Department of Biology, Norwegian University of Science and Technology, Trondheim, Norway

ORCID IDs: 0000-0003-4756-1203 (PB); 0000-0003-4408-8262 (NS); 0000-0001-6572-3232 (FK); 0000-0002-6657-8740 (JH); 0009-0001-5393-6609 (JL); 0000-0002-5947-6367 (DS); 0000-0003-2388-7655 (YL); 0000-0002-6540-8520 (MK); 0000-0002-3692-7487 (RH)

***Corresponding author**: renier.vanderhoorn@biology.ox.ac.uk

ABSTRACT

Most angiosperms recognise the flg22 epitope in bacterial flagellin via homologs of cell surface receptor FLS2 and mount pattern-triggered immune responses. However, flg22 is buried within the flagellin protein and logic and preliminary experiments have indicated that proteases might be required for flg22 release. Here, we demonstrate that the extracellular subtilase SBT5.2 processes flg22 from its precursor in the apoplast of *Nicotiana benthamiana*. Interestingly, however, SBT5.2 also inactivates the immunogenicity of flagellin and flg22 by preferentially cleaving within the flg22 epitope, consistent with previous reports that flg22 is unstable in the apoplast. The prolonged lifetime of flg22 in *sbt5.2* mutants results in increased bacterial immunity in priming assays, indicating that SBT5.2 counterbalances flagellin immunogenicity to provide spatial-temporal control and restrict costly immune responses to the infection site. Since flagellin can bind to FLS2 and flg22 is stabilised when bound to FLS2, we propose that SBT5.2 might process flagellin when bound to FLS2 to produce a flg22-FLS2 complex that can recruit BAK1 and trigger immune signalling. Counterbalancing flagellin immunogenicity is conserved across the plant kingdom, given the conservation of both SBT5.2 and the cleavage site within flagellin and the observation that very similar processing events occur in the apoplast of tomato and Arabidopsis.

Keywords: Plant immunity, *Pseudomonas syringae*, flagellin, subtilases, flg22, *Nicotiana benthamiana*.

INTRODUCTION

Bacterial flagellin is a strong inducer of innate immune responses in both plants and animals. The flagellum enables bacterial motility and is a polymer that consists of thousands of flagellin proteins in a tubular assembly (Chevance & Hughes 2008; Gomez-Gomez & Boller 2002; Ramos et al., 2004; Samatey et al., 2001). The surface of the flagellum is glycosylated with *O*-glycans that can differ in composition between bacterial strains (Chiku et al. 2013).

In most angiosperms, recognition of bacterial flagellin is mediated by a cell surface localised receptor kinase called FLS2 (flagellin sensing-2, Gómez-Gómez & Boller, 2000). FLS2 recognizes a highly conserved epitope of 22-amino acids in the N-terminal region of flagellin, called flg22 (Felix et al., 1999; Zipfel et al., 2004). The flg22 peptide is routinely used to trigger pattern-triggered immunity (PTI), but how flg22 is made available during infection is not yet clear.

It has been predicted that to expose flg22, the flagellin protein needs to be processed from its monomeric precursor because the flg22 epitope is not fully exposed in the flagellin monomer, and is unlikely to bind the FLS2 receptor in this conformation (Chen et al., 2024). Indeed, a protease inhibitor cocktail can suppress the perception of flagellin, but not of flg22 (Buscaill et al., 2019). A recent report describes that Arabidopsis subtilases SBT5.2 and SBT1.7 are processing flagellin at the C-terminus of flg22 (Matsui et al., 2024). However, despite the reduced processing of flagellin in *sbt5.2/sbt1.7* mutants, these mutants only show a 2-minute delay in the maximum release of reactive oxygen species (ROS). And although a hampered flagellin perception should have increased bacterial susceptibility, bacterial growth assays on *sbt5.2/sbt1.7* mutants have not been reported.

Here, we describe how flagellin is quickly inactivated in the apoplast of the model plant *Nicotiana benthamiana* by subtilase SBT5.2 and other proteases. In addition to processing flg22 from its precursor, SBT5.2 more quickly inactivates the immunogenic activity of flagellin by preferentially cleaving in the middle of the flg22 epitope. Indeed, *sbt5.2* mutants show an increased stability of flagellin and flg22 in the apoplast, associated with prolonged immunogenicity. Consequently, *sbt5.2* mutants are less susceptible to bacterial colonisation when primed with low flg22 concentrations, indicating that SBT5.2 provides spatial-temporal control over immune responses to restrict the induction of costly defence responses.

RESULTS

Monomeric flagellin is immunogenic and quickly degraded in the apoplast.

To study the processing of flagellin in the apoplast, we isolated flagella from *Pseudomonas syringae* pv. *tabaci* 6605 (*Pta*6605) and produced polymeric and monomeric flagellin. We next incubated this with apoplastic fluid (AF) isolated from *N. benthamiana* and separated the proteins on protein gels to monitor the degradation of flagellin in AF over time. Monomeric flagellin rapidly degrades in AF within minutes, whereas polymeric flagellin remains stable in AF for over 24 hours (**Figure 1A**), consistent with the hypothesis that polymeric flagellin is protected from degradation.

To investigate the stability of flagellin immunogenicity in the apoplast, flagellin monomers and polymers were incubated in AF for 30 and 60 minutes and added to leaf discs of *N. benthamiana* to measure the release of reactive oxygen species (ROS) by measuring luminescence in a plate reader. Monomeric flagellin triggered a strong ROS burst when added immediately to leaf discs, whereas polymeric flagellin only triggered a weak oxidative burst (**Figure 1B**). This weak response might originate from flagellin monomers that may have dissociated from the polymer. However, the oxidative burst quickly disappears when flagellin is incubated with AF for 30 or 60 minutes before treating leaf discs (**Figure 1C**), indicating that the immunogenicity of flagellin monomers quickly disappears in the apoplast.

Flagellin is degraded by apoplastic proteases

To further investigate flagellin processing in AF, we employed liquid chromatography-tandem mass spectrometry (LC-MS/MS) to analyse the peptides released from flagellin when incubated in AF. We identified a total of 466 different flagellin-derived peptides, spanning the entire protein sequence except for peptides containing the six *O*-glycosylation sites of flagellin (**Figure 2A,** Buscaill et al., 2019; Taguchi et al., 2006), indicating that monomeric flagellin is not fully deglycosylated before it is processed into peptides. Indeed, peptides covering this region were detected upon incubation of nonglycosylated flagellin from the flagellin glycosyl transferase mutant *Δfgt1* when incubated in AF (Supplemental **Figure S1**).

The detected peptides released from *Pta*6605 flagellin assemble into seven clusters (**Figure 2A,** purple line). This peptide distribution pattern suggests that flagellin undergoes cleavage at specific sites by endopeptidases and that exopeptidases subsequently remove residues from the N- and C-termini, supported by endopeptidases that remove N- and C-terminal peptides.

Closer inspection of the protein coverage indicates that flagellin might be cleaved by endopeptidase(s) at LSTS↓M↓TRLS, LQIA↓TKITS↓QIRGQT↓MAIK, ILQR↓MREL↓AV↓QSRN and EFRA↓M↓SSEL (**Figure 2A**), of which the first two processing regions would release flg22 from its precursor.

Because we detect a loss of immunogenicity of flagellin, we searched for putative processing sites within the flg22 sequence and found two candidate regions: LKIN↓SAKD, SAKD↓DAAG (**Figure 2A**). Processing in either of these sites would inactivate the elicitor activity (Felix et al., 1999). Collectively, the putative cleavage sites do not have an obvious consensus sequence.

We next mapped the putative cleavage sites onto a model of the structure of the flagellin monomer. The putative cleavage sites distribute over the hinge region and various positions in α-helixes that are not exposed in polymeric glycosylated flagellin (**Figure 2B**), explaining why monomeric flagellin is more susceptible to proteolysis than polymeric flagellin.

To confirm the cleavage events within flagellin, we designed and custom-synthesised quenched peptides (Qps) containing different cleavage sites, flanked by an N-terminal quencher (DABCYL) and a C-terminal fluorophore (Glu-EDANS). Processing these peptides releases a fluorophore that is detected by fluorescence (**Figure 2C**). The Qps cover the two sites within flg22 (LKIN↓SAKD (Qp2) and SAKD↓DAAG (Qp3)); the flg22-flanking sites STSM↓TRLS (Qp1) and LQIA↓TKITS (Qp4), as well as one additional obvious putative processing site following the flg22 sequence (RGQT↓MAIK (Qp5)). Incubation of these Qps

in AF causes a rapid increase of fluorescence when compared to the water control (**Figure 2D**), indicating that these peptides are cleaved in AF. These data also indicate that Qp1 and Qp2 are more efficiently cleaved in AF compared to the other three Qps.

Flagellin is processed by apoplastic subtilases

To identify the class of proteases responsible for processing flagellin, we isolated AFs from leaves overexpressing protease inhibitors *Pi*Epi1, *Sl*Cys8 and *Hs*TIMP, which inhibit subtilases (SBTs), papain-like Cys proteases (PLCPs) and metalloproteases, respectively (Tian et al., 2004; Jutras et al., 2016; Grosse-Holz et al., 2019). Incubation of these AFs with quenched peptides revealed that *Pi*Epi1 blocks processing of all QPs, whereas *Hs*TIMP only suppresses Qp3 processing and *Sl*Cys8 and had no effect (**Figure 3A**). Qp1 processing is less efficiently blocked by *Pi*Epi1, indicating that this site is cleaved by a protease different from an *Pi*Epi1-sensitive subtilase. The near complete blockage of Qp4 processing by PiEpi1 indicates that only subtilases cleave at this region. Processing of Qp3 is suppressed more by *Pi*Epi1 than by *Hs*TIMP, again indicating that Qp3 is processed by subtilases rather than other proteases. These results indicate that subtilases are responsible for most of the flagellin processing in AF.

We next tested if *Pi*Epi1 can reduce the inactivation of immunogenicity in AF by incubating flagellin or flg22 in AF for 40 minutes and measuring their ability to trigger the oxidative burst. Importantly, immunogenic activity was detected after incubation of flagellin or flg22 peptide with AFs isolated from leaves transiently expressing *Pi*Epi1, but not from the EV control (**Figure 3B**), indicating that subtilases are responsible for degrading the immunogenicity of both flagellin and flg22.

SBT5.2 subtilases are required for degrading flagellin and inactivating flg22

The *N. benthamiana* genome encodes for 72 putative subtilases (Kourelis et al., 2019; Beritza et al., 2024). Among the ten subtilases detected in the apoplast, four are notably more abundant: SBT5.2a, SBT1.9a, SBT1.7a, and SBT1.7c (Jutras et al., 2018; Sueldo et al., 2023; Beritza et al., 2024), also referred to as SBT1-4, respectively (Puchol Tarazona et al., 2021). To identify the subtilase responsible for flagellin processing, we depleted transcripts of these four subtilases using Virus-Induced Gene Silencing (VIGS) with Tobacco Rattle Virus (TRV) vectors carrying 300 bp fragments targeting these subtilases. Each fragment was designed to target one subtilase, except for the fragment present in *TRV::SBT5.2*, which targets the three SBT5.2 homologs (a-c) for which transcripts were detected in *N. benthamiana* (Supplemental **Figure S2**; Beritza et al., 2024).

To determine which subtilases are required for processing the quenched peptides, Qps were incubated with AFs isolated from *TRV::SBT* plants and fluorescence was measured. Processing of all Qps except Qp1 was significantly reduced in the AF of *TRV::SBT5.2* plants compared to the *TRV::GFP* control (**Figure 4A**). The absence of reduced Qp1 processing is consistent with the observation that Qp1 processing is also less sensitive to inhibition by *Pi*Epi1 and indicates that Qp1 is not processed by abundant, *Pi*Epi1-sensitive subtilases. Qp3 processing is not as strongly reduced in *TRV::SBT5.2* plants compared to the other Qps, whereas Qp3 processing was also reduced in AF isolated from *TRV::SBT1.9a* and *TRV::SBT1.7a* plants. This

is consistent with SBT1.9a being a phytaspase (Kourelis et al., 2019; Reichardt et al., 2018), which prefer cleaving after aspartic residues present in Qp3 (SAKDDAAG). Taken together, these results indicate that SBT5.2s seem to be responsible for processing Qps 2-5 but Qp3 is also cleaved by phytaspase SBT1.9a and SBT1.7a. Qp1 processing is unaffected by silencing the four tested subtilases.

Since SBT5.2s seem responsible for processing flg22 at sites 2 and 3, we tested the stability of flg22 immunogenicity by incubating flg22 for various times in AF isolated from *TRV::SBT5.2* and *TRV::GFP* plants. Importantly, the decline of flg22 immunogenicity is much slower in AF of *TRV::SBT5.2* plants compared to *TRV::GFP* plants (**Figure 4B**), indicating that SBT5.2s are responsible for quickly inactivating flg22.

Increased stability of flagellin and flg22 in AF of *sbt5.2* plants

To further investigate the role of SBT5.2 in flagellin processing, we took advantage of two recently described *sbt5.2* triple mutant lines of *N. benthamiana*, which are disrupted in the open reading frames encoding all three *SBT5.2* genes (Beritza et al., 2024). Activity-based profiling with FP-TAMRA on AF demonstrates that the *sbt5.2* mutants lack the most active subtilases at 70 kDa (**Figure 5A**), consistent with being the most active subtilase in AF of *N. benthamiana* (Jutras et al., 2018; Puchol Tarazona et al., 2021; Sueldo et al., 2023).

To test if flagellin processing is altered in these mutants, we incubated purified flagellin protein in AF isolated from WT and *sbt5.2* mutant plants and analysed flagellin degradation by western blot. Notably, flagellin was more stable in the AF of both *sbt5.2* mutants than in the AF of WT plants (**Figure 5B**), demonstrating robustly that SBT5.2s are necessary for flagellin processing. Interestingly, in addition to the full length flagellin protein we also detect the accumulation of several intermediate flagellin degradation products in AF of *sbt5.2* plants, suggesting that other proteases slowly process flagellin in the absence of SBT5.2s.

Consistent with flagellin protein degradation, also the immunogenicity of the flg22 peptide is less reduced in AF of *sbt5.2* plants. The flg22 peptide retains immunogenicity longer when incubated in AF isolated from *sbt5.2* plants, whereas flg22 immunogenicity is lost when incubated with AF of WT plants (**Figure 5C**).

To confirm the reduced flg22 processing in *sbt5.2* plants, we also tested processing of the quenched peptides. Remarkably, processing of Qp1, Qp2 and Qp5 is significantly reduced in AF of *sbt5.2* mutant plants (**Figure 5D**). Qp3 processing is only slightly reduced in AF of *sbt5.2* mutant plants, whereas Qp4 processing is strongly reduced but not significant (**Figure 5D**), However, all Qps are still cleaved to some extend in the absence of *sbt5.2*, suggesting that other protease in AF might slowly process these peptides in the absence of SBT5.2s.

SBT5.2 processes flagellin and inactivates flg22 *in vitro*

To determine if SBT5.2 is sufficient for processing flagellin and inactivating flg22, we purified SBT5.2a-His from agroinfiltrated plants using Nickel-NTA agarose (Beritza et al. 2024). Increased concentrations of SBT5.2a-His result in the accumulation of more active isoforms that are labelled with the activity-based probe for Ser hydrolases (FP-TAMRA, **Figure 6A**). Incubation of increasing amounts of purified SBT5.2a-His with the flagellin protein confirmed that flagellin can be processed by SBT5.2 (**Figure 6B**).

Furthermore, incubation of flg22 with different concentrations of purified SBT5.2a-His resulted in a dose-dependent inactivation of flg22 elicitor activity (**Figure 6B**). Incubation of purified SBT5.2a-His with the quenched peptides revealed that Qp2 is the best substrate and that Qp1, Qp4 and Qp5 are SBT5.2a substrates but that Qp3 is hardly cleaved (**Figure 6C**). Taken together, these data demonstrate that purified SBT5.2a-His is sufficient to process flagellin and inactivate flg22 by cleaving the LKINSAKD motif, consistent with the observed peptide coverage.

SBT5.2 processes flagellin monomers stepwise

Having purified SBT5.2a-His, we studied flagellin processing in more detail. First, we tested if SBT5.2a can only act on flagellin monomer and not polymers. We produced flagellin monomers from the polymer and used a 100 kDa molecular cut-off filter to separate the monomer from the polymer. Incubation of purified SBT5.2a-His with each of these samples demonstrated that SBT5.2 is unable to process the flagellin polymer and rapidly processes the monomer (**Figure 7A**).

The observation of various processing intermediates in **Figure 6B** and **Figure 7A** suggests that purified SBT5.2a-His cleaves flagellin monomers at multiple positions. To study flagellin processing over time, we monitored flagellin processing (35 kDa, including glycans) by SBT5.2a-His over time using western blot analysis. The time course revealed that the fragments appear in a distinct order (**Figure 7B**). First, a 31 kDa fragment appears at 10 minutes (**Figure 7B**). Then, at 30 minutes, three additional fragments appear of 29, 28 and 26 kDa (**Figure 7B**). Finally, at 60 minutes, the 31, 29 and 28 kDa fragments have disappeared and besides the 26 kDa fragment, a 25 kDa fragment accumulates (**Figure 7B**). An additional 23 kDa fragment was detected upon incubation with 2-fold more SBT5.2a-His (**Figure 6B**). Collectively, these data suggest that SBT5.2a-His might prefer a cleavage site that releases 31 kDa fragment first and then slowly processes this fragment by additional cleavages in the N-terminal half of processed flagellin.

SBT5.2s dampens flg22-induced immune responses

To determine the outcome of SBT5.2 depletion on bacterial growth, we performed infection assays on plants depleted for subtilases with *Pseudomonas syringae*. Bacterial growth on leaves transiently expressing *Pi*Epi1 is significantly reduced (**Figure 8A**), indicating that subtilases might collectively reduce the immunogenicity of flagellin or act in immune signaling. However, bacterial growth was unaltered in *TRV::SBT5.2* compared to control plants (**Figure 8B**), and in *sbt5.2* mutant lines compared to WT plants (**Figure 8C**).

The absence of bacterial growth phenotypes on the *sbt5.2* mutant, despite the prolonged stability of flagellin and flg22 in these mutants, prompted us to test if priming by higher flg22 levels can induce immune responses that can be detected in bacterial growth assays. Strong effects on bacterial growth are normally shown by pre-treating (priming) tissues with 1 µM flg22 (Zipfel et al., 2004; Tsuda et al., 2009). We reasoned that the effect of SBT5.2 depletion could only be shown at threshold flg22 concentrations because higher concentrations would trigger antibacterial immunity irrespective of SBT5.2. Importantly, both WT and *sbt5.2* mutant plants respond equally to various concentrations of flg22 (**Figure 8D** and Supplemental **Figure S4**), indicating that SBT5.2 depletion did not alter flg22 perception by *Nb*FLS2. We therefore monitored bacterial

growth in leaves pre-treated with 1, 10 and 100 nM flg22. As expected, pre-treatment of WT plants with 100 nM flg22 reduces bacterial growth compared to pre-treatments with 1 and 10 nM flg22, indicating that these low flg22 concentrations are below the threshold to induce antibacterial immunity (**Figure 8E**). In both *sbt5.2* mutants, however, pre-treatment with 10 nM flg22 reduces bacterial growth whereas no altered bacterial growth was detected upon pre-treatment with 1 and 100 nM flg22 (**Figure 8E**). Further experiments showed that antibacterial immunity is reduced in *sbt5.2* mutant plants also upon pre-treatment with 5 nM flg22, but not with 20 nM flg22 (Supplemental **Figure S5**). These data demonstrate that SBT5.2 dampens antibacterial immunity by inactivating the immunogenicity of flg22 at low flg22 concentrations.

DISCUSSION

Flagellin and flg22 are almost universally recognized by angiosperm plants. Here, we demonstrated that extracellular SBT5.2 subtilases mediate the quick inactivation of the immunogenicity of both flg22 and flagellin by cleaving in the middle of the flg22 sequence. The increased stability of flg22 in *sbt5.2* mutant plants reduces bacterial growth at low flg22 concentrations, suggesting that SBT5.2 contributes to a spatial-temporal dampening of immunity to restrict the immune responses to the infection site. We also demonstrate that abundant apoplastic subtilases are responsible for these and other flagellin processing events and that the polymeric flagellin is protease resistant.

Flagellin monomers are quickly processed

We demonstrated that flagellin monomers exhibit proteolytic sensitivity in both apoplastic fluids and in the presence of purified SBT5.2a-His, in contrast to the flagellin polymers, which are stable. This is consistent with the notion that the discovered processing sites in flagellin monomers are concealed when part of the polymer. The only solvent-exposed regions of flagellin within the polymer are covered with *O*-glycans, which seem to protect the polymer against proteases (Taguchi et al., 2006; Buscaill et al., 2019). Monomeric flagellin is essential for perception because the flg22 epitope is concealed within the flagellin polymer. Monomeric flagellin can have different sources. First, monomeric flagellin is produced in the bacterial cell and kept unfolded through its interaction with its chaperone FliS (Auvray et al., 2001). This pre-polymerised flagellin could escape into the apoplast, similar to cytoplasmic EF-Tu and CSP proteins that are also perceived in the apoplast (Kunze et al., 2004; Felix et al., 2003). Second, some flagellin monomers may fail to polymerise when secreted through the flagellin tubule during flagella synthesis but most of this is prevented by the flagellim cap protein, FliD (Yonekura et al., 2000). Indeed, the *fliD* mutant of *Pta*6604 secreted large amounts of monomeric flagellin and triggers strong immune responses (Shimizu et al., 2003). Third, flagella are shed upon starvation and during the cell cycle (Zhu & Gao 2020; Kint & Viollier 2023; Yonekura et al., 2000; Kostyukova et al., 1988), and although flagella do not depolymerise (Aizawa et al., 1990), they might release monomers when incubated in an apoplastic environment. Fourth, damage of the flagellin filament, e.g. by BGAL1 removing the terminal mVio residue from the glycan, may initiate the release of flagellin monomers from within the filament (Buscaill et al., 2019).

Release of immunogenic peptides from flagellin

Our data indicates that cleavage site-1 and site-4 would release immunogenic flagellin fragments from flagellin. N-terminal processing of flg22 at site-1 is suppressed by subtilase inhibitor *Pi*Epi1 but is not significantly suppressed when silencing *SBT5.2, SBT1.9,* or *SBT1.7s*. Site-1 processing is, however, significantly reduced in the *sbt5.2* mutant and purified SBT5.2a-His can cleave Qp1, indicating that SBT5.2 can process flagellin at the N-terminal site of the flg22 epitope. C-terminal processing at site-4 is suppressed by *Pi*Epi1 and upon silencing *SBT5.2*. Site-4 processing is also reduced in the *sbt5.2* mutant, although not significantly, and purified SBT5.2a-His can cleave Qp4. Taken together, these data indicate that SBT5.2 could cleave flagellin at both ends of flg22 and release flg22 from its precursor. These data are consistent with the recent report that SBT5.2 in Arabidopsis processes at site-4 in the flagellin of *Pto*DC3000 (Matsui et al., 2024).

Subtilases preferentially cleave flagellin within the flg22 epitope at two sites

Our data indicates that flagellin is quickly processed by subtilases cleaving at site-2 and site-3 in the flg22 epitope. This is consistent with the fact that we did not detect the full length flg22 immunogenic peptide in MS experiments. Site-2 (LKIN↓SAKD) is mostly cleaved by SBT5.2 because processing of Qp2 is drastically reduced upon *SBT5.2* silencing and in *sbt5.2* mutants. Qp2 is also a very good substrate of purified SBT5.2a-His. Site-3 processing is probably mostly caused by SBT1.9 and SBT1.7a because Qp3 processing is significantly reduced upon silencing *SBT1.9* and *SBT1.7a*. Qp3 is not efficiently processed by purified SBT5.2a-His and is not significantly reduced in *sbt5.2* mutants, indicating that at this site is not preferred by SBT5.2 but that SBT5.2 might still cleave this region because it is such an abundant subtilase. Processing at site-3 (SAKD↓DAAG) by SBT1.9 is consistent with its annotation as a phytaspase, which cleave after Asp residues (Reichardt et al., 2018). Interestingly, the recent description of flagellin processing in Arabidopsis seedling exudates indicates that flagellin of *Pto*DC3000 is also processed at site-2 and that this is reduced in seedling exudates of *sbt5.2/sbt1.7* mutants (Matsui et al., 2024), indicating that processing of flagellin within the flg22 epitope might occur universally. Indeed, we detected the same site-2 processing with apoplastic fluids from tomato (Supplemental **Figure S6**), indicating that flagellin processing within the flg22 epitope will occur in many plant species.

Our data indicates that site-2 is preferentially cleaved within flagellin because Qp2 is preferentially processed in apoplastic fluids (**Figure 2C**) and by purified SBT5.2a-His (**Figure 6C**). Analysis of the time course of flagellin processing by purified SBT5.2 indicates that flagellin is first processed by SBT5.2 into a 31 kDa fragment, before smaller intermediates accumulate (**Figure 7C**). This indicates that flagellin immunogenicity is predominantly inactivated by subtilases in the apoplast, and that the release of flg22 is not a dominant process.

The preferred processing at site-2 is also supported by modelling of flagellin with SBT5.2a by AlphaFold Multimer (AFM, Evans et al., 2021). The best model predicts that the catalytic Ser residue is proximate to the site-2 cleavage site such that the S2 and S4 substrate binding pockets in SBT5.2a are occupied by Ile38 (P2) and Leu36 (P4) of flagellin, respectively (Supplemental **Figure S7**). Interestingly, this AFM

model indicates that the flagellin monomer would fold on the flg22 hinge to expose this processing site to SBT5.2a (Supplemental **Figure S7**).

FLS2 may stabilise the flg22 epitope to support flg22 release from flagellin

The quick inactivation of flagellin and flg22 by SBT5.2 cleaving within the flg22 epitope counterbalances the perception of flagellin and flg22 (**Figure 9**). The perception of both flagellin and flg22 in *N. benthamiana* demonstrates that at least some unprocessed flagellin/flg22 must have reached FLS2 and activated PTI signalling. The perception of flagellin/flg22 by FLS2 is possibly mediated by a high affinity for binding FLS2, indicating that sufficient flagellin/flg22 can bind FLS2 before being cleaved. One caveat in this and our studies is that the preparation of flagellin monomer includes a heat or low-pH treatment, which might denature flagellin and expose flg22.

Importantly, flagellin was found to effectively compete with radiolabeled flg22 (IC50 = 120 nM), in microsomal fractions that presumably lack subtilases (Meindl et al., 2000). However, although flagellin can bind FLS2, it is unclear at this stage if it would also activate FLS2 signalling because that would require subsequent BAK1 binding to FLS2. The extension of flg22 at its C-terminus is likely to obstruct BAK1 binding, based on the structure of flg22 bound to the FLS2 and BAK1 (Sun et al., 2013). This indicates that SBT5.2 and other proteases might be required to degrade flagellin whilst the flg22 epitope is protected by FLS2 (**Figure 9**). Indeed, it has also been shown that binding of flg22 to membranes stabilises the peptide (Meindl et al, 2000), which is consistent with the fact that the cleavage site for SBT5.2 would be obstructed upon binding FLS2 (Sun et al., 2013). This process might explain the 2-minute delay detected in perceiving flagellin compared to flg22 (Matsui et al., 2024), and would indicate that SBT5.2 counterbalances flagellin perception by inactivating flagellin before it is perceived, whilst also facilitating flagellin perception when it is bound to FLS2.

Redundancies in the extracellular proteolytic machinery

Although flg22 and flagellin are more stable in apoplastic fluids of *sbt5.2* plants, they are still slowly degraded. Likewise, processing of quenched peptides is significantly reduced, but not absent in apoplastic fluids of the *sbt5.2* mutant, or in apoplastic fluids from leaves expressing *Pi*Epi1. These data indicate that proteases other than SBT5.2, or even *Pi*Epi1 insensitive proteases, contribute to flagellin processing in the apoplast. Indeed, the apoplast contains dozens of active Ser and Cys proteases, as well as aspartic proteases (pepsins) and metalloproteases (Grosse-Holz et al., 2018; Jutras et al., 2019). This suggests that the apoplast is a highly digestive microenvironment, where many proteases collectively contribute to a redundant proteolytic machinery that control levels of immunogenic peptides. The redundancy in the extracellular proteolytic machinery might explain why flagellin is still perceived in the *sbt5.2* mutant. Alternatively, flagellin processing is not required in case BAK1 can assemble with the flagellin-FLS2 complex without flagellin processing. The latter mechanism is similar to how flagellin is recognised on the cell surface receptor by TLR5 in animals (Yoon et al., 2012).

SBT5.2 may confer temporal-spatial control of antibacterial immunity

We demonstrated that flg22 and flagellin immunogenicity is prolonged in *sbt5.2* mutants and that this is associated with increased antibacterial immunity when *sbt5.2* mutants are pre-treated with low flg22 concentrations (5-10 nM flg22). These data indicate that SBT5.2 dampen immune responses both temporally and spatially to avoid the costly indication of antibacterial immunity in tissues that are not or no longer exposed to sufficient bacteria. Interestingly, this mechanism may not be restricted to flagellin perception in *N. benthamiana*, as similar processing of the flg22 epitope has been detected in seedling exudates of Arabidopsis (Matsui et al., 2024) and apoplastic fluids of tomato (Supplemental **Figure S6**). This mechanism is probably also universal because the cleavage sites within the flg22 epitope are highly conserved across bacteria (Supplemental **Figure S8**), and one can speculate that bacteria evolved cleavage sensitivity in flagellin to avoid recognition. In addition, SBT5.2a is well-conserved across plant species (Beritza et al. 2024) and frequently detected in the apoplast. The role of SBT5.2 in spatial-temporal control of elicitor levels may also extend to other elicitor proteins. Indeed, we recently found that SBT5.2 is also responsible for reducing levels of csp22 epitope in Cold Shock Proteins (CSPs) of *P. syringae* (Chen et al., 2024), and SBT5.2 also quickly inactivates the elf18 peptide elicitor (Supplemental **Figure S9**). Collectively, these data indicate that a conserved extracellular proteolytic machinery consisting of SBT5.2 and other proteases provides spatial-temporal control on elicitor peptide levels to restrict the induction of costly defence responses.

MATERIALS and METHODS

Plants materials and growth conditions - *Nicotiana benthamiana* plants were grown in a growth chamber at 22°C and ~60% relative humidity with a 16-hour photoperiod and a light intensity of 2000 cd·sr m−2.

Agroinfiltration - *Agrobacterium tumefaciens* GV3101 (pMP90) was used for agroinfiltration of *N. benthamiana*. Agrobacteria were grown in Luria-Bertani (LB) medium with 25 µg/ml rifampicin and 50 µg/ml kanamycin at 28°C. For transient expression of proteins in *N. benthamiana*, overnight cultures of Agrobacterium carrying binary vectors were harvested by centrifugation. Bacterial cells were resuspended in agroinfiltration buffer (10 mM $MgCl_2$, 10 mM MES pH 5.6, 150 µM acetosyringone) at an OD_{600} of 0.5. After 1 h at 28°C, cells were infiltrated into leaves of 4-wk-old *N. benthamiana*. The infected plants were grown in a growth chamber until use.

Quenched peptides - The quenched peptides (Qps) from flagellin were commercially synthesized with a DABCYL N-terminal modification and a Glu-EDANS C-terminal modification (GenScript, Piscataway, New Jersey, United States) at a purity of 95% (Supplemental **Table S3**). There were resuspended in DMSO at a concentration of 1 mM. This stock solution was further diluted in water to a concentration of 200 µM. AFs or purified SBT5.2a were mixed with QPs at a final concentration of 10 µM in a volume of 100 µl, and fluorescence was measured immediately at 21ºC using an Infinite M200 plate reader (Tecan, Mannedorf, Switzerland) every minute over 5 min with an excitation wavelength of 335 nm and emission wavelength of 493 nm.

Virus-induced Gene Silencing (VIGS) – Agrobacterium cultures were grown overnight and resuspended in agroinfiltration buffer at OD_{600} = 0.5. Agrobacteria carrying binary plasmids for expressing

RNA2 of TRV carrying silencing fragments (Supplemental **Table S1**) were mixed 1:1 with Agrobacteria containing TRV1 (Liu et al. 2002). After incubation for 1 hour at 21°C, the mixed cultures were infiltrated into the leaves of 14-day-old *N. benthamiana* plants. The infiltrated plants were grown for another 4 to 5 weeks in a growth chamber until use.

Apoplastic Fluids (AFs) isolation - *N. benthamiana* leaves were submerged in ice-cold water and vacuum infiltrated in a 50 ml syringe with a plunger. The surface of water-infiltrated leaves was dried with absorbing paper and leaves were carefully inserted into an empty 20 ml syringe, which was placed in a 50 ml tube. AFs were collected by centrifugation at 2,000 *g* at 4°C for 10 min. AFs were immediately used or frozen using liquid nitrogen and stored at -20°C until use.

Labelling of flagellin - The purified flagellin was labelled using an amine-reactive dye (DyLight® 488 NHS Ester; Thermo 46402) accordingly to manufacturer's instructions. The mix was incubated for one hour in the dark at room temperature. Excess dye was removed by loading the labelling mix into a column (Amicon® Ultra 0.5 centrifugal filter devices 3K; Merck UFC500324) and centrifuged for 8 minutes at 10,000 x g. After loading another 100 µl PBS, the column was centrifuged for 8 minutes at 10,000 x g. The above step was repeated, the column was transferred upside-down into a new tube and centrifuged for 5 minutes. The labelled flagellin was kept in dark at 4°C and used within a month.

SDS-PAGE and Western blot - The protein samples were mixed with 4x gel loading buffer (200 mM Tris-HCl (pH6.8), 400 mM DTT, 8% SDS, 0.4% bromophenol blue, 40% glycerol) and heating at 90°C for 5 min. The samples were loaded on 15% SDS-PAGE and separated at 180V in Invitrogen Novex vertical gel tanks. The Amersham® Typhoon was used to measure fluorescence (Cy2: 488 nm for labelled flagellin, Cy5: 685 nm for ladder). The proteins were also visualised by total protein staining with Instant Blue® Coomassie Protein Stain (Abcam ab119211). For Western blot analysis, proteins were transferred onto a polyvinylidene difluoride (PVDF, BioRad) membrane using BioRad Trans-blot Turbo® according to the manufacturer's instructions (BioRad Kit 1704275). Blots were blocked for 1 hours at 21°C or overnight at 4°C with 5% (w/v) skim milk in PBS-T (PBS tablets; Merck 524650, 0.1% Tween-20; Merck P1379). The membrane was incubated with 1:5000 anti-flagellin antibody (Taguchi et al. 2003) in 5% (w/v) skim milk for one hours at 21°C. 1:5000 anti-flagellin antibody was added in the 5% (w/v) skim milk in PBS-T for one hours at 21°C. Blots were washed twice with PBS-T for 5 minutes, and incubated with 1:5000 HRP-conjugated anti-goat antibody in PBS-T for 1 hours at 21°C. Blots were washed four times with PBS-T for 5 minutes and chemiluminescent signals were detected using Clarity Western ECL Substrate (BioRad,), and visualised using the ImageQuant® LAS-4000 imager (GE Healthcare, Healthcare Life Sciences, Little Chalfont, UK).

SBT5.2a-His purification - Four-week-old *N. benthamiana* leaves were infiltrated with a 1:1 mixture (final OD600 = 0.5 for each) of Agrobacterium tumefaciens GV3101 containing the silencing suppressor P19 and pPB097 (Chen et al., 2024). Apoplastic fluid containing SBT5.2a-His was extracted 6 days after infiltration and purified as previously described (Schuster et al., 2022; Homma et al., 2023).

ROS assays - ROS assays were performed as described previously (Buscaill et al., 2019).

Mass spectrometry - To generate samples for the analysis of endogenously digested peptides, 10ng/µl of purified flagellin of *Pta*6605 or *Pta*6605Δ*fgt1* was incubated for 30 min or 60 min with apoplastic fluids

isolated from leaves of *N. benthamiana*, or tomato (Money Maker Cf0), or purified SBT5.2a-HIS at 21°C (the specific condition is indicated under each figure). The samples were supplemented (AF and/or the purified proteins) with four volumes of MS-grade acetone. After incubating the mixture was kept on ice for 1 hour, and subjected to centrifugation at 18,000 x g for 20 minutes. Following centrifugation, four-fifths of the supernatants was transferred to fresh Eppendorf tubes and the acetone was evaporated using vacuum centrifugation. The dried peptide samples were sent to the Analytics Core Facility Essen (ACE) for MS analysis.

AlphaFold Multimer – All models were generated using AFM v2.1.1 (Evans et al., 2021; Jumper et al., 2021) on the Advanced Research Computing (ARC) clusters as described in Homma et al., 2023. Briefly, the sequences of mature flagellin and SBT5.2 catalytic domain were submitted to model the structure. Database preset was set to 'full_dbs' to include the full bfd database for multi-sequence alignment search for all predictions. For flagellin monomer, 'monomer_ptm' was specified for the '--model_preset' flag to obtain pTM confidence measure. Monomer pTM score was extracted from the .pkl output file specific to the model.

Phylogenetic analysis **–** Flagellin sequences were collected for various Pseudomonas strains. Clustal Omega (Sievers & Higgins, 2018) was used for amino acid sequence alignment and neighbour-joining tree construction. The tree was visualised using iTOL (Letunic & Bork, 2024) and displayed with midpoint rooting.

Activity-Based Protein Profiling (ABPP) - FP-TAMRA (Thermo-Fisher) was prepared as 10 µM stock solutions in dimethyl sulfoxide (DMSO). Serine hydrolase labelling was performed as described previously with minor modifications (Kaschani et al., 2009). Briefly, apoplastic fluids were incubated with 0.2 µM FP-TAMRA (Thermo Fischer) in PBS buffer pH7 for 1h at 21°C in the dark. Labelling was stopped by adding 4x gel loading buffer (200 mM Tris-HCl (pH6.8), 400 mM DTT, 8% SDS, 0.4% bromophenol blue, 40% glycerol) and heating at 90°C for 5 min. The proteins were separated on SDS-PAGE and fluorescently labelled proteins were detected by in-gel scanning with the Typhoon FLA 9000 (GE Healthcare Life Sciences) using Cy3 settings (532nm excitation and 610PB filter).

Infection assays - flg22 peptides were diluted in water. *N. benthamiana* plants were infiltrated with the different concentrations of flg22 peptide or with water as a mock control. *N. benthamiana* plants were infiltrated when 3-4 weeks-old, and 3 fully expanded leaves were infiltrated per plant. 24h later, infiltrated leaves were infiltrated with 10^5 CFU/ml *Pta*6605. The next day (1 dpi), three leaf discs were punched with a cork borer from each infected leaf, and surface-sterilised with 15% hydrogen peroxide for 2 minutes. Leaf discs were then washed twice in MilliQ and dried under sterile conditions. Leaf discs were placed into a 1.5 ml safe-lock Eppendorf tube with three 3 mm diameter metal beads and 1 ml of MilliQ. Tubes were placed in tissue lyser for five minutes at 30 Hertz/second. 200 µl of the lysed tissue was transferred to the first row (A) of a 96-well plate and then serial 10-fold dilutions were made until the last row (20 µl tissue + 180 µl MilliQ). 20 µl of undiluted tissue and serial dilutions were plated on LB-agar plates containing *Pseudomonas* CFC Agar Supplement (Oxoid SR0103). Plates were allowed to dry, incubated at 28ºC for two days and then colonies were counted. The p-value was calculated using the two-tailed Student t-test to compare bacterial growth between leaves from WT and *sbt5.2* mutant plants.

Funding: This project was financially supported by BBSRC 17RM3 project BB/R017913/3 'GH35' (PB) and 19RM3 project BB/015128/1 'Galactosyrin' (PB, NS); ERC-2020-AdG project 101019324 'ExtraImmune' (JH, RH); BBSRC Interdisciplinary Bioscience DTP project DDT00230 (JL); the National Natural Science Foundation of China (No. 32070289 to YL) and the Chinese Academy of Sciences Scholarship (YL).

Acknowledgements: We like to thank Ben Excel for his help with purifying flagellin; Yuki Ichinose for providing the anti-flagellin antibody; Urszula Pyzio for excellent plant care; and Sarah Rodgers, Patricia Bowman and Caroline O'Brien for excellent technical support.

Author contributions: PB and RH conceived the project; PB and NS performed most of the experiments; FK and MK performed proteomic analysis; PB and JH performed experiments with purified SBT5.2; PB and DS analysed susceptibility of *TRV::SBT5.2* plants; JL added AlphaFold Multimer models; PB and YL performed bacterial growth assays on *sbt5.2* plants; PB and RH wrote the manuscript with input of all authors.

REFERENCES

Aizawa SI, Vonderviszt F, Ishima R, Akasaka K. (1990) Termini of Salmonella flagellin are disordered and become organized upon polymerization into flagellar filament. *J. Mol. Biol.* **211**, 673-677.

Beritza, K., Buscaill, P., Song, S., Jutras, P. V., Huang, J., Mach, L., Dong, S., and Van der Hoorn, R. A. L. (2024) SBT5.2s are the major active extracellular subtilases processing IgG antibody 2F5 in the *N. benthamiana* apoplast. *bioRxiv doi.org/10.1101/2024.04.07.588497*.

Buscaill P, Chandrasekar B, Sanguankiattichai N, Kourelis J, Kaschani F, Thomas EL, Morimoto K, Kaiser M, Preston GM, Ichinose Y, van der Hoorn RAL. (2019) Glycosidase and glycan polymorphism control hydrolytic release of immunogenic flagellin peptides. *Science* **364**, eaav0748.

Chen C, van der Hoorn RAL, Buscaill P. (2024) Releasing hidden MAMPs from precursor proteins in plants. *Trends Plant Sci.* **29**, 428-436.

Chen C, Buscaill P, Sanguankiattichai N, Huang J, Kaschani F, Kaiser M, Van der Hoorn RAL (2024) Extracellular plant subtilases dampen cold shock peptide elicitor levels. *Submitted manuscript.*

Chevance FF, Hughes KT. (2008) Coordinating assembly of a bacterial macromolecular machine. *Nat. Rev. Microbiol.* **6**, 455-465.

Chiku K, Yamamoto M, Ohnishi-Kameyama M, Ishii T, Yoshida M, Taguchi F, Ichinose Y, Ono H. (2013) Comparative analysis of flagellin glycans among pathovars of phytopathogenic *Pseudomonas syringae*. *Carbohydr. Res.* **375**, 100-104.

Evans, R., O'Neill, M., Pritzel, A., Antropova, N., Senior, A., Green, T., Žídek, A., Bates, R., Blackwell, S., Yim, J., Ronneberger, O., Bodenstein, S., Zielinski, M., Bridgland, A., Potapenko, A., Cowie, A., Tunyasuvunakool, K., Jain, R., Clancy, E., Kohli, P., Jumper, J., & Hassabis, D. (2021) Protein complex prediction with AlphaFold-Multimer. *bioRxiv* 2021.10.04.463034.

Felix G, Boller T. (2002) Molecular sensing of bacteria in plants. The highly conserved RNA-binding motif RNP-1 of bacterial cold shock proteins is recognized as an elicitor signal in tobacco. *J Biol Chem.* **278**, 6201-6208.

Felix G, Duran JD, Volko S, Boller T. (1999) Plants have a sensitive perception system for the most conserved domain of bacterial flagellin. *Plant J.* **18**, 265-276.

Gómez-Gómez L, Boller T. (2000) FLS2: an LRR receptor-like kinase involved in the perception of the bacterial elicitor flagellin in Arabidopsis. *Mol Cell.* **5**, 1003-1011.

Gómez-Gómez L, Boller T. (2002) Flagellin perception: a paradigm for innate immunity. *Trends Plant Sci.* **7**, 251-256.

Grosse-Holz F, Kelly S, Blaskowski S, Kaschani F, Kaiser M, van der Hoorn RAL. (2018) The transcriptome, extracellular proteome and active secretome of agroinfiltrated *Nicotiana benthamiana* uncover a large, diverse protease repertoire. *Plant Biotechnol J.* **16**, 1068-1084.

Grosse-Holz F, Madeira L, Zahid MA, Songer M, Kourelis J, Fesenko M, Ninck S, Kaschani F, Kaiser M, van der Hoorn RAL. (2018) Three unrelated protease inhibitors enhance accumulation of pharmaceutical recombinant proteins in *Nicotiana benthamiana. Plant Biotechnol. J.* **16**, 1797-1810.

Homma F, Huang J, van der Hoorn RAL. (2023) AlphaFold-Multimer predicts cross-kingdom interactions at the plant-pathogen interface. *Nat Commun.* **14**, 6040.

Jumper J, Evans R, Pritzel A, Green T, Figurnov M, Ronneberger O, Tunyasuvunakool K, Bates R, Žídek A, Potapenko A, Bridgland A, Meyer C, Kohl SAA, Ballard AJ, Cowie A, Romera-Paredes B, Nikolov S, Jain R, Adler J, Back T, Petersen S, Reiman D, Clancy E, Zielinski M, Steinegger M, Pacholska M, Berghammer T, Bodenstein S, Silver D, Vinyals O, Senior AW, Kavukcuoglu K, Kohli P, Hassabis D. (2021) Highly accurate protein structure prediction with AlphaFold. *Nature* **596**, 583-589.

Jutras PV, Grosse-Holz F, Kaschani F, Kaiser M, Michaud D, van der Hoorn RAL. (2019) Activity-based proteomics reveals nine target proteases for the recombinant protein-stabilizing inhibitor SlCYS8 in *Nicotiana benthamiana*. *Plant Biotechnol J.* **17**, 1670-1678.

Jutras PV, Marusic C, Lonoce C, Deflers C, Goulet MC, Benvenuto E, Michaud D, Donini M. (2016) An accessory protease inhibitor to increase the yield and quality of a tumour-targeting mAb in *Nicotiana benthamiana* leaves. *PLoS One* **11**, e0167086.

Kaschani F, Gu C, Niessen S, Hoover H, Cravatt BF, van der Hoorn RAL. (2009) Diversity of serine hydrolase activities of unchallenged and botrytis-infected *Arabidopsis thaliana*. *Mol. Cell. Proteomics* **8**, 1082-1093.

Kint N, Viollier PH. (2023) Extracellular transfer of a conserved polymerization factor for multi-flagellin filament assembly in Caulobacter. *Cell Rep.* **42**, 112890.

Kostyukova AS, Pyatibratov MG, Filimonov VV, Fedorov OV. (1988) Flagellin parts acquiring a regular structure during polymerization are disposed on the molecule ends. *FEBS Lett.* **241**, 141-144.

Kourelis J, Kaschani F, Grosse-Holz FM, Homma F, Kaiser M, van der Hoorn RAL. (2019) A homology-guided, genome-based proteome for improved proteomics in the alloploid *Nicotiana benthamiana*. *BMC Genomics* **20**, 722.

Kunze G, Zipfel C, Robatzek S, Niehaus K, Boller T, Felix G. (2004) The N terminus of bacterial elongation factor Tu elicits innate immunity in Arabidopsis plants. *Plant Cell* **16**, 3496-3507.

Letunic I, Bork P. (2024) Interactive Tree of Life (iTOL) v6: recent updates to the phylogenetic tree display and annotation tool. *Nucleic Acids Res.* **13**, gkae268.

Matsui S, Noda S, Kuwata K, Nomoto M, Tada Y, Shinohara H, Matsubayashi Y. (2024) Arabidopsis SBT5.2 and SBT1.7 subtilases mediate C-terminal cleavage of flg22 epitope from bacterial flagellin. *Nat. Commun.* **15**, 3762.

Meindl T, Boller T, Felix G. (2000) The bacterial elicitor flagellin activates its receptor in tomato cells according to the address-message concept. *Plant Cell* **12**, 1783-1794.

Puchol Tarazona AA, Maresch D, Grill A, Bakalarz J, Torres Acosta JA, Castilho A, Steinkellner H, Mach L. (2021) Identification of two subtilisin-like serine proteases engaged in the degradation of recombinant proteins in *Nicotiana benthamiana*. *FEBS Lett*. **595**, 379-388.

Ramos HC, Rumbo M, Sirard JC. (2004) Bacterial flagellins: mediators of pathogenicity and host immune responses in mucosa. *Trends Microbiol.* **12**, 509-517.

Reichardt S, Repper D, Tuzhikov AI, Galiullina RA, Planas-Marquès M, Chichkova NV, Vartapetian AB, Stintzi A, Schaller A. (2018) The tomato subtilase family includes several cell death-related proteinases with caspase specificity. *Sci. Rep.* **8** 10531.

Samatey FA, Imada K, Nagashima S, Vonderviszt F, Kumasaka T, Yamamoto M, Namba K. (2001) Structure of the bacterial flagellar protofilament and implications for a switch for supercoiling. *Nature* **410**, 331-337.

Schuster M, Eisele S, Armas-Egas L, Kessenbrock T, Kourelis J, Kaiser M, van der Hoorn RAL. (2024) Enhanced late blight resistance by engineering an EpiC2B-insensitive immune protease. *Plant Biotechnol J.* **22**, 284-286.

Shimizu R, Taguchi F, Marutani M, Mukaihara T, Inagaki Y, Toyoda K, Shiraishi T, Ichinose Y. (2003) The DeltafliD mutant of *Pseudomonas syringae* pv. *tabaci*, which secretes flagellin monomers, induces a strong hypersensitive reaction (HR) in non-host tomato cells. *Mol Genet Genomics.* **269**, 21-30.

Sievers F, Higgins DG. (2018) Clustal Omega for making accurate alignments of many protein sequences. *Protein Sci.* **27**, 135-145

Sueldo DJ, Godson A, Kaschani F, Krahn D, Kessenbrock T, Buscaill P, Schofield CJ, Kaiser M, van der Hoorn RAL. (2024) Activity-based proteomics uncovers suppressed hydrolases and a neo-functionalised antibacterial enzyme at the plant-pathogen interface. *New Phytol.* **241**, 394-408.

Sun Y, Li L, Macho AP, Han Z, Hu Z, Zipfel C, Zhou JM, Chai J. (2013) Structural basis for flg22-induced activation of the Arabidopsis FLS2-BAK1 immune complex. *Science* **342**, 624-628.

Taguchi F, Shimizu R, Nakajima R, Toyoda K, Shiraishi T, Ichinose Y. (2003) Differential effects of flagellins from *Pseudomonas syringae* pv. *tabaci*, *tomato* and *glycinea* on plant defense response. *Plant Physiol. Biochem.* **41**, 165-174.

Taguchi F, Takeuchi K, Katoh E, Murata K, Suzuki T, Marutani M, Kawasaki T, Eguchi M, Katoh S, Kaku H, Yasuda C, Inagaki Y, Toyoda K, Shiraishi T, Ichinose Y. (2006) Identification of glycosylation

genes and glycosylated amino acids of flagellin in *Pseudomonas syringae* pv. *tabaci*. *Cell Microbiol.* **8**, 923-938.

Tian M, Huitema E, Da Cunha L, Torto-Alalibo T, Kamoun S. (2004) A Kazal-like extracellular serine protease inhibitor from *Phytophthora infestans* targets the tomato pathogenesis-related protease P69B. *J. Biol. Chem.* **279**, 26370-26377.

Tsuda K, Sato M, Stoddard T, Glazebrook J, Katagiri F. (2009) Network properties of robust immunity in plants. *PLoS Genet.* **5**, e1000772.

Yonekura K, Maki S, Morgan DG, DeRosier DJ, Vonderviszt F, Imada K, Namba K. (2000) The bacterial flagellar cap as the rotary promoter of flagellin self-assembly. *Science* **290**, 2148-2152.

Yoon SI, Kurnasov O, Natarajan V, Hong M, Gudkov AV, Osterman AL, Wilson IA. (2012) Structural basis of TLR5-flagellin recognition and signaling. *Science* **335**, 859-864.

Zhu S, Gao B. (2020) Bacterial flagella loss under starvation. (2020) *Trends Microbiol.* **28**, 785-788.

Zhuang XY, Lo CJ. (2020) Construction and loss of bacterial flagellar filaments. *Biomolecules* **10**, 1528.

Zipfel C, Robatzek S, Navarro L, Oakeley EJ, Jones JD, Felix G, Boller T. (2004) Bacterial disease resistance in Arabidopsis through flagellin perception. *Nature* **428**, 764-767.

FIGURES

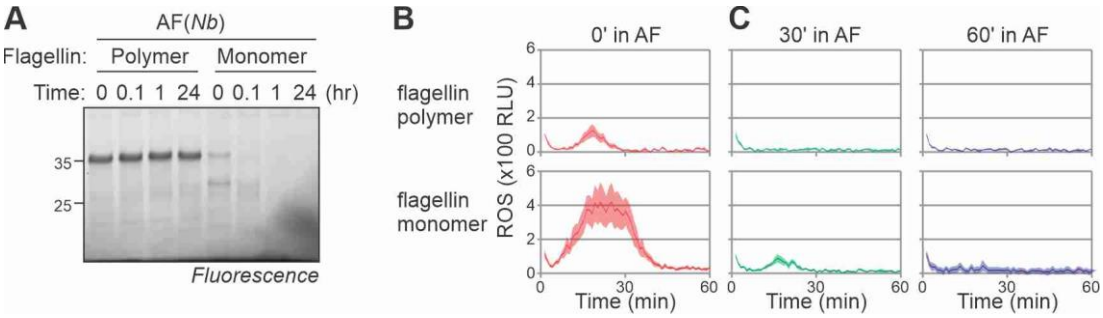

Figure 1. Monomeric flagellin is quickly processed and inactivated in *N. benthamiana* apoplast.

(A) Monomeric but not polymeric flagellin is quickly degraded in the apoplast of *N. benthamiana*. Purified polymeric flagellin from *Pta*6605 bacteria was monomerised and incubated with apoplastic fluids (AF) isolated from *N. benthamiana* leaves for 0, 0.1, 1 or 24 hrs and samples were analysed on a protein gel by fluorescence scanning. **(B)** Polymeric flagellin some has minor immunogenicity which disappears when incubated in AF. **(C)** Monomeric flagellin is immunogenic but this is quickly inactivated in AF. (B-C) 10 µg/ml of polymeric and monomeric flagellin were incubated with AF for 0, 30 or 60 minutes. Treated samples were added to leaf discs floating on luminol and horse radish peroxidase (HRP) and ROS release was monitored using a luminescence plate reader for 60 minutes. Error shades represent SE of n=6 biological replicates. RLU, relative luminescence units.

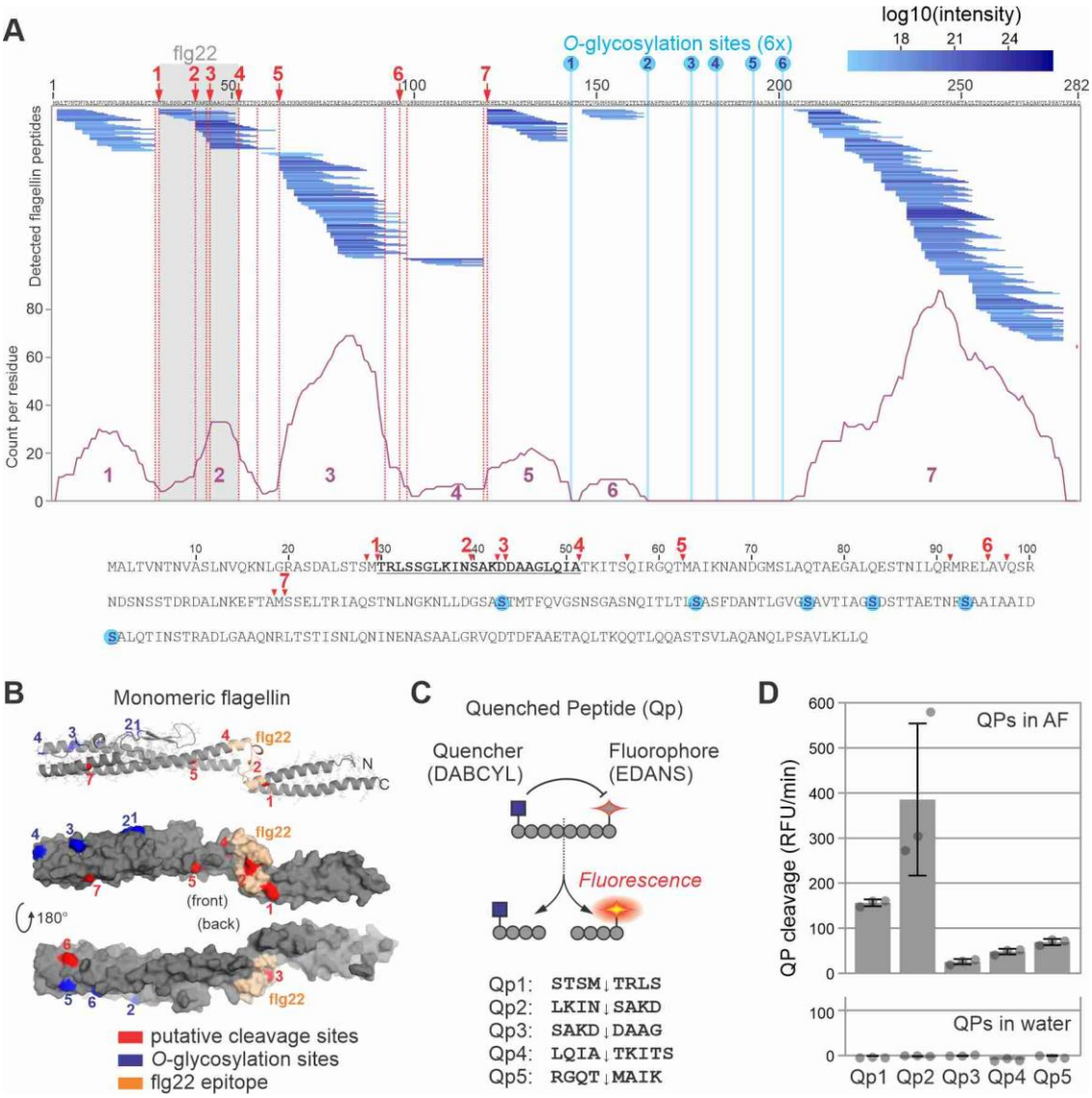

Figure 2 Flagellin is degraded by apoplastic proteases.

(A) Degradation products of flagellin in AF detected by LC-MS/MS analysis. Purified flagellin was incubated with AF isolated from *N. benthamiana* leaves. Proteins were precipitated with 80% acetone and the supernatant (peptide fraction) was analysed by LC-MS/MS. All flagellin-derived peptides detected were matched to the flagellin protein sequence. Highlighted are the flg22 sequence (grey), putative cleavage sites (red dashed lines) and six *O*-glycosylation sites (light blue lines). The number of times each residue was detected in the peptides is indicated with the purple graph, showing the peptides belong to seven clusters. Below: position of the putative cleavage sites within the flagellin protein sequence. Highlighted are flg22 (grey), putative cleavage sites (red) and the six *O*-glycosylation sites (blue). **(B)** Location of putative cleavage sites within the predicted structure of the flagellin monomer, generated with AlphaFold. Highlighted are the putative cleavage sites (red), and the *O*-glycosylation sites (blue). **(C)** Concept of using quenched peptides (Qps) to monitor processing. Qp cleavage separates the fluorophore from the quencher, resulting in fluorescence. Qps containing the cleavage regions in flagellin were custom-synthesised. **(D)** Qps are processed in AF. Qps were mixed with water or AF and fluorescence was measured immediately over 5 min. Error bars represent SE of n=3 different AFs.

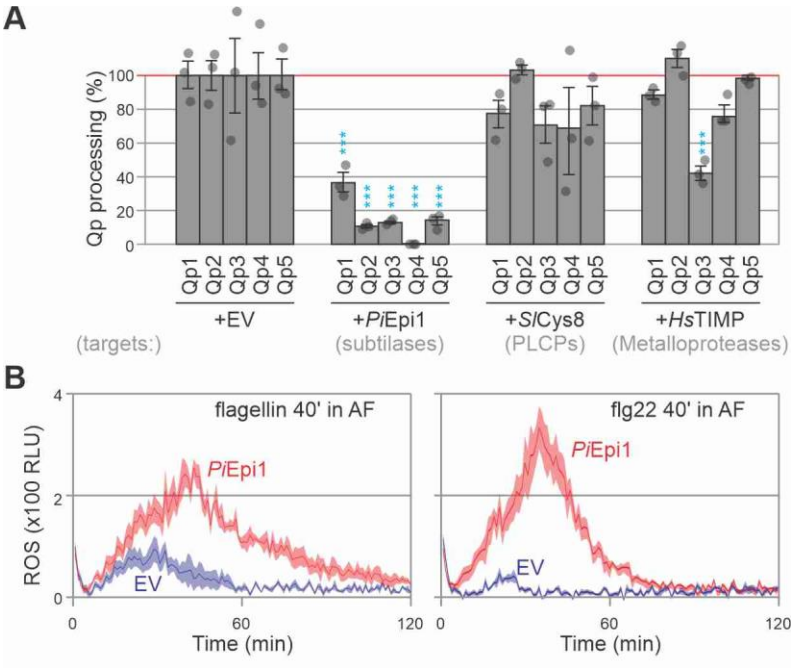

Figure 3. Subtilase-inhibitor *Pi*Epi1 suppresses processing of Qps, flg22 and flagellin.

(A) Subtilase inhibitor *Pi*Epi1 suppresses processing of all quenched peptides (Qps). Apoplastic fluids (AFs) isolated from *N. benthamiana* leaves transiently expressing protease inhibitors *Pi*Epi1, *Sl*Cys8 and *Hs*TIMP were mixed with Qps and fluorescence and was immediately monitored using a plate. Qp processing in the empty vector (EV) control was set at 100% for each Qp. Error bars represent ±SE of n = 3 biological replicates (i.e., AFs from 3 plants). **(B)** *Pi*Epi1 increases immunogenicity of monomeric flagellin and flg22. AFs from plants transiently expressing *Pi*EPi1 or the empty vector (EV) control were incubated with 10 µg/ml monomeric flagellin or 100 nM flg22 for 40 min and then added to leaf discs of *N. benthamiana* plants floating on luminol and horse radish peroxidase (HRP). ROS release was measured for 120 minutes by luminescence (relative light units, RLU) using a plate reader. Error shades represent SE of n=6 replicates. RLU, relative luminescence units.

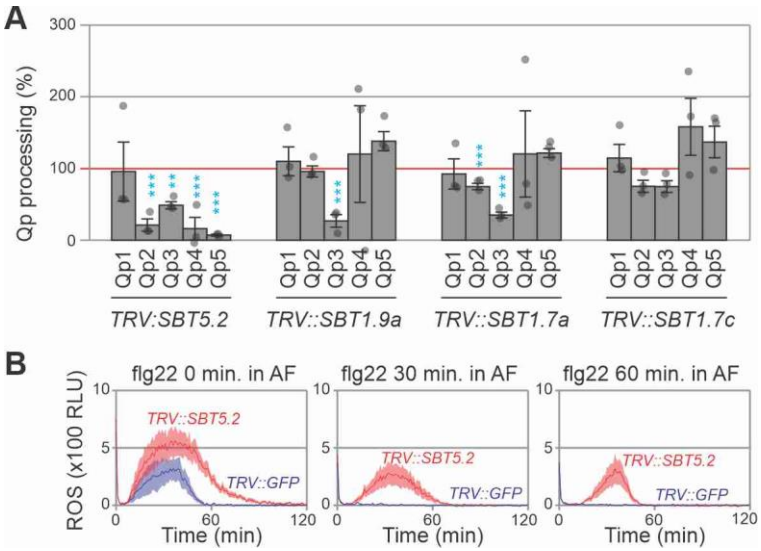

Figure 4. SBT5.2 is required for processing Qps 2-5 and inactivating flg22.

(A) SBT5.2 is required for Qp processing in AF. AF from plants silenced for various subtilases were mixed with 10 µM quenched peptides and fluorescence was monitored immediately using a plate reader. Qp processing in AF of *TRV::GFP* control plants was set at 100%. Error bars represent SE of n=3 different plants. **(B)** *SBT5.2* silencing reduces the degradation of flg22 immunogenicity. 100 nM flg22 was incubated in AF from *N. benthamiana* for 0, 30 and 60 minutes before adding to leaf discs from *N. benthamiana* floating in HRP or luminol. Luminescence was measured and plotted against time. Error shades indicate SE of n=6 replicates. RLU, relative luminescence units.

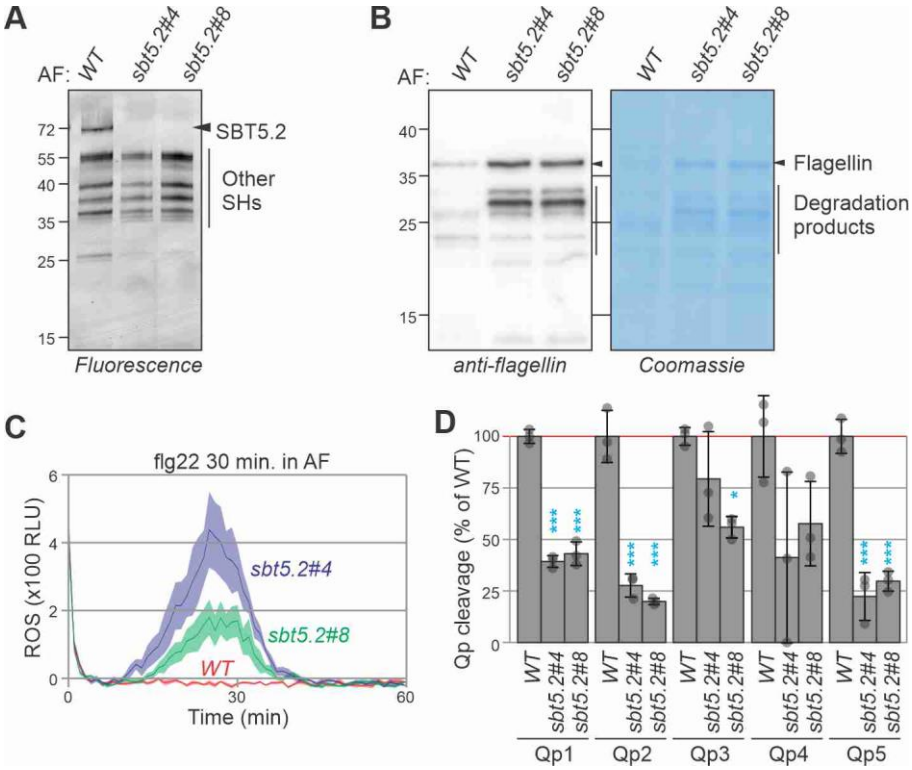

Figure 5 *sbt5.2* mutants show reduced flagellin, flg22 and processing of quenched peptides.

(A) SBT5.2s are the major active subtilases in the apoplast. AF was isolated from WT plants and two triple *sbt5.2* mutants and serine hydrolases (SHs) were labeled with FP-TAMRA and detected by in-gel fluorescence scanning. **(B)** Reduced flagellin processing in the *sbt5.2* mutants. Purified flagellin was incubated for 30 min with AF from leaves of WT or two *sbt5.2* mutants. The samples were separated on SDS-PAGE and stained with coomassie or analysed by western blotting using anti-flagellin antibodies. **(C)** flg22 inactivation is reduced in AF isolated from both *sbt5.2* triple mutants. AF from leaves of WT or *sbt5.2* mutant plants were incubated with 100 nM flg22 peptide for 30 minutes then added to *N. benthamiana* leaf discs floating on luminol-HRP solution. The ROS burst was monitored using a luminescence plate reader. Error shades represent SE of n=6 biological replicates. RLU, relative luminescence units. **(D)** Qp processing is reduced in AF isolated from both *sbt5.2* triple mutants. 10 µM Qps were incubated with AF of WT or *sbt5.2* mutants and fluorescence was measured with a plate reader. Error bars represent SE of n=4 samples.

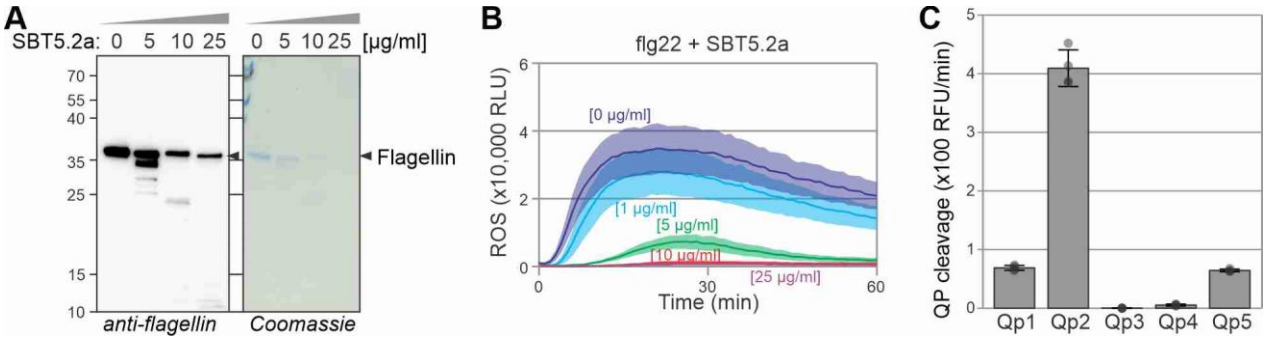

Figure 6. Purified SBT5.2a degrades flagellin and inactivates flg22.

(A) Purified SBT5.2a-His processes flagellin. Purified flagellin was incubated with various concentrations of purified SBT5.2a for 30 minutes and samples were separated on SDS-PAGE and stained with Coomassie or analysed by western blotting using anti-flagellin antibodies. **(B)** Purified SBT5.2a-His inactivates the flg22 elicitor. 50 nM flg22 was incubated with various concentration of purified SBT5.2a-His for 30 minutes. These samples were added to leaf discs of *N. benthamiana* plants floating on luminol-HRP solution and the ROS burst was monitored using a luminescence plate reader. Error shades represent SE of n=6 biological replicates. RLU, relative luminescence units. **(C)** Purified SBT5.2a-His cleaves Qps. Qps were incubated with 10 µl of 25 µg/ml purified SBT5.2a-His and fluorescence was measured. Error bars indicate SE of n=4 replicates.

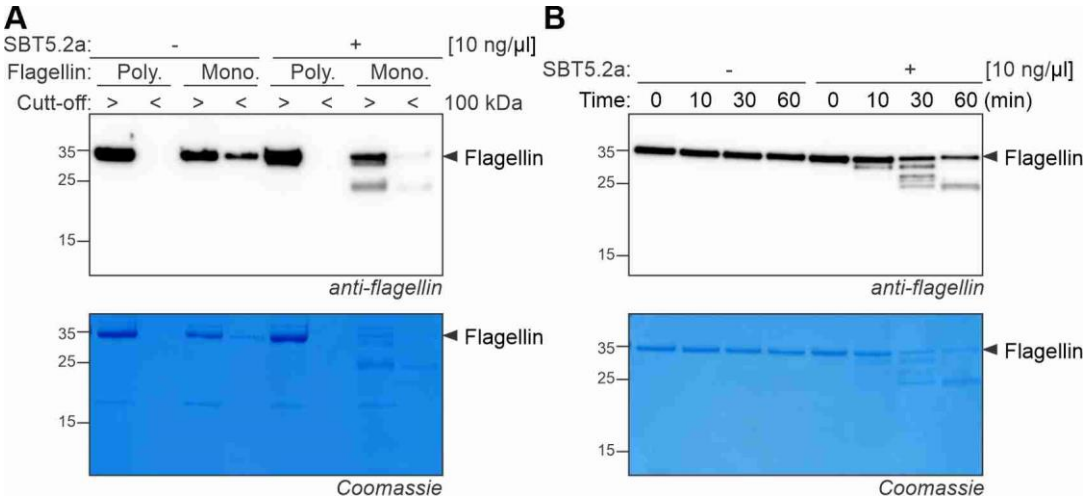

Figure 7. SBT5.2 processes monomeric flagellin into several intermediates.

(A) SBT5.2a cannot process polymeric flagellin. Purified flagellin was monomerised by heat treatment and both polymeric and monomeric flagellin was passed through a 100 kDa MW cut-off filter. The flow-through (<100 kDa) and the residue (>100 kDa) for each sample was incubated for 30 min with or without 10 µg/ml purified SBT5.2a-His. The samples were separated on 15% SDS-PAGE and stained with Coomassie or analysed by western blotting using anti-flagellin antibodies. **(B)** Purified SBT5.2 processes flagellin in distinct steps. Purified flagellin was incubated for 0, 10, 30, 60 min with or without 10 µg/ml purified SBT5.2a-His. The samples were separated on 15% SDS-PAGE and stained with coomassie or analysed by western blotting using anti-flagellin antibodies.

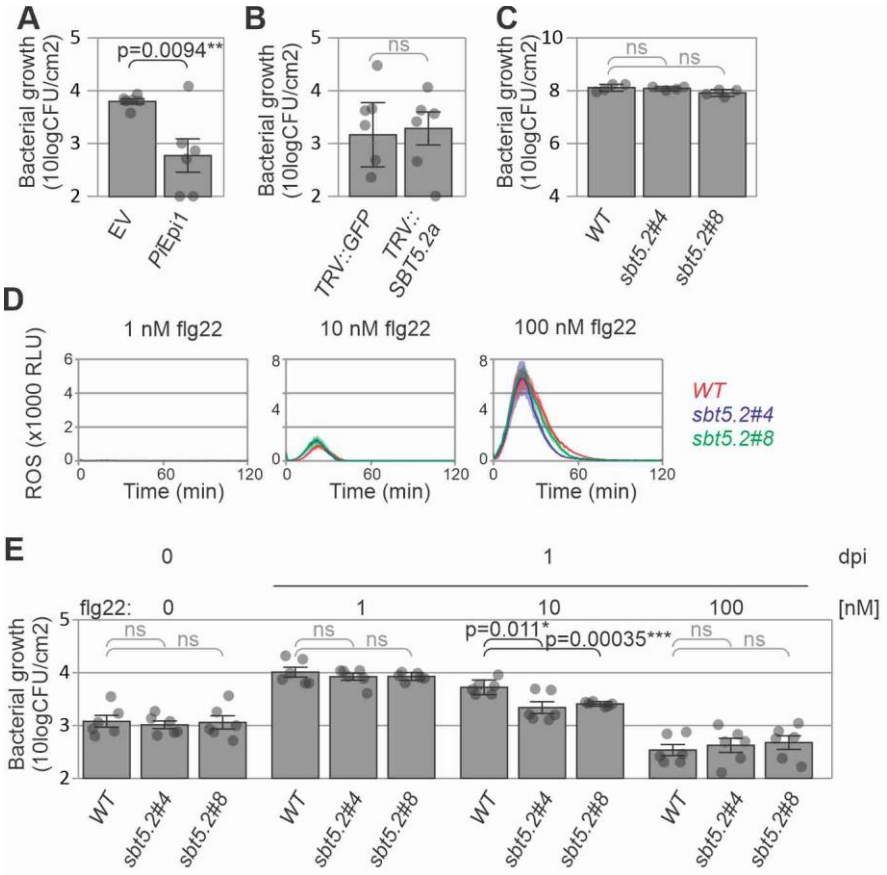

Figure 8 SBT5.2s dampens elicitor levels to reduce antibacterial immunity.

(A) Leaves transiently expressing *Pi*Epi1 have increased antibacterial immunity. Agroinfiltrated leaves expressing empty vector (EV) or *Pi*Epi1 were sprayed with *Pta*6605 at day-3 post agroinfiltration and bacterial growth was measured three days later. Error bars represent SE of n=6 biological replicates. The p-value was calculated using the two-tailed Student t-test. **(B)** *SBT5.2* silenced plants have no altered susceptibility to *Pta*6605. *TRV::GFP* and *TRV::SBT5.2* plants were spray-infected with *Pta*6605 and bacterial growth was determined at 3dpi. Error bars represent SE of n=3 biological replicates. **(C)** The *sbt5.2* plants have no altered susceptibility to *Pto*DC3000(*ΔhQ*). Plants were spray inoculated with *Pto*DC3000(*ΔhQ*) and bacterial growth was determined at 3dpi. Error bars represent STDEV of n=4 replicates. **(D)** No altered response to flg22 in *sbt5.2* mutants. Leaf discs from 4-week-old *N. benthamiana* WT or *sbt5.2* mutants floating on luminal-HRP were treated with 1, 10 or 100 nM flg22 and ROS burst was monitored using a plate reader. Error shades represent SE of n=6 biological replicates. **(E)** Immune priming by low flg22 concentrations increases in *sbt5.2* mutant plants. Leaves of 4-week-old WT and *sbt5.2* mutant plants were infiltrated with 1, 10 or 100 nM flg22 or water. After 24 hours incubation, the leaves were infiltrated with $1x10^5$ bacteria/ml *Pta*6605. Colony forming units (CFUs) were determined one day post infection (dpi). Error bars represent SE of n=6 replicates.

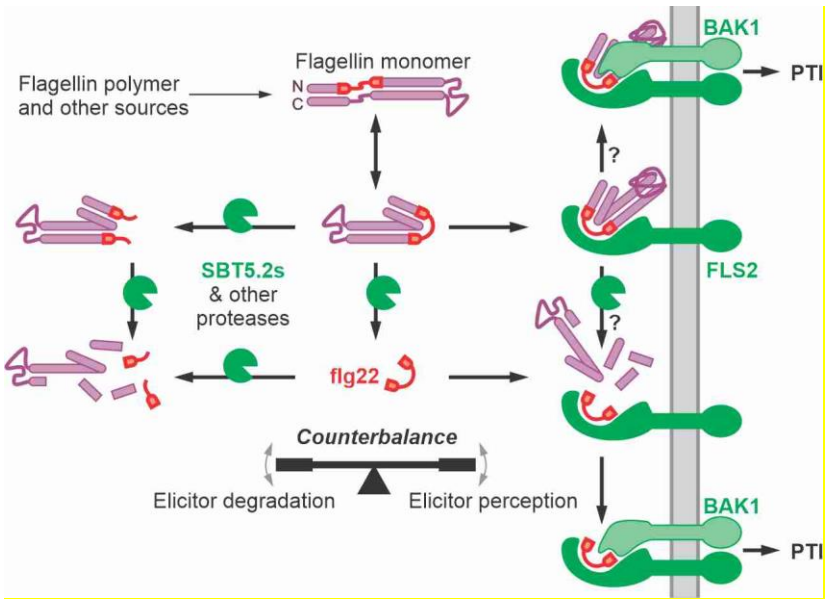

Figure 9 SBT5.2 counterbalances elicitor perception and inactivation.

Elicitor activity of both flagellin and flg22 is quickly inactivated by SBT5.2s and other proteases cleaving in the middle of the flg22 epitope, yet sufficient flg22 may be released and bind FLS2. Flagellin protein can bind to FLS2 and may associate with BAK1 to trigger immunity without requiring processing. Alternatively, FLS2 may stabilise the flg22 epitope by binding flagellin and SBT5.2s and other proteases may process flagellin to facilitate BAK1 association and subsequent immune signalling. PTI, pattern-triggered immunity; PM, plasma membrane.